Biogeosciences Discuss., doi:10.5194/bg-2016-202, 2016
Manuscript under review for journal Biogeosciences
Published: 19 May 2016

Biogeosciences Discussions
Open Access
EGU

1

2 # MONODEUTERATED METHANE:
3 # AN ISOTOPIC PROBE TO MEASURE BIOLOGICAL METHANE METABOLISM
4 # RATES AND TRACK CATABOLIC EXCHANGE REACTIONS

Jeffrey J. Marlow[1*#], Joshua A. Steele[1^], Wiebke Ziebis[2], Silvan Scheller[1],
David Case[1], Victoria J. Orphan[1]

[1] Division of Geological and Planetary Sciences, California Institute of Technology, Pasadena, CA, 91125 USA
[2] Department of Biological Science, University of Southern California, Los Angeles, CA, 90089 USA
* Current address: Dept. of Organismic and Evolutionary Biology, Harvard University, Cambridge, MA 02138 USA
^ Current address: Southern California Coastal Water Research Project, Costa Mesa, CA 92626 USA
# Correspondence email: marlow@fas.harvard.edu

5

Biogeosciences Discuss., doi:10.5194/bg-2016-202, 2016
Manuscript under review for journal Biogeosciences
Published: 19 May 2016

Biogeosciences Discussions Open Access EGU

Abstract

Biological methane oxidation is a globally relevant process that mediates the flux of an important greenhouse gas through both aerobic and anaerobic metabolic pathways. However, measuring the rates of these metabolisms presents many obstacles, from logistical barriers to regulatory hurdles and poor precision. Here we present a new approach for measuring rates of microbial methane metabolism that is non-toxic, rapid, and relatively high throughput, alleviating some of the current methodological challenges. Specifically, we tested the potential for using monodeuterated methane (CH_3D) as a metabolic substrate for measuring the rate of methane activation by quantifying the change in the aqueous D/H ratio over time using a water isotope analyzer. This method represents a non-toxic, comparatively rapid and straightforward approach that is complementary to existing radio (^{14}C)- and stable (^{13}C) carbon isotopic methods; by probing hydrogen atom dynamics, it offers an additional dimension through which to examine the rates and pathways of methane metabolism. We provide direct comparisons between the CH_3D procedure and the well-established $^{14}CH_4$ radiotracer approach for several methanotrophic systems, including type I and type II aerobic methanotroph cultures, and methane seep sediment and carbonate rocks under anoxic and oxic incubation conditions. We also employ this method to investigate the role of pressure on methane oxidation rates in anoxic seep sediment, revealing an 80% increase at the equivalent of ~900 m water depth (40 MPa).

The monodeuterated methane approach offers a procedurally straightforward, reliable method that advances three specific aims: 1) the direct comparison of methane oxidation rates between different experimental treatments of the same inoculum; 2) the determination of an absolute scaling factor using paired CH_3D and ^{14}C-radiocarbon procedures for new systems of interest; and 3) a continued evaluation of C- and H-atom tracking through methanotrophic

Biogeosciences Discuss., doi:10.5194/bg-2016-202, 2016
Manuscript under review for journal Biogeosciences
Published: 19 May 2016

metabolisms, with specific foci on enzyme reversibility and anabolic/catabolic branch points. The procedural advantages, consistency, and novel research questions enabled by the monodeuterated methane method should prove useful in a wide range of culture-based and environmental microbial systems to further elucidate methane metabolism dynamics.

1. Introduction

Methane-consuming microbial processes represent an important component of biogeochemical cycles in natural freshwater and marine environments, as well as in human-impacted systems. In terrestrial soils, methane production in rice fields, anoxic wetlands, and thawing permafrost supports methanotrophic communities (Holzapfel-Pschorn et al., 1985; Mackelprang et al., 2011). In marine settings, an estimated 85 Tg of methane per year, derived from biogenic and thermogenic sources, enters the subseafloor, the vast majority of which is anaerobically consumed in anoxic sediments (Reeburgh, 2007). Much of what remains is taken up in microoxic or oxic zones of the sediment or water column by aerobic methanotrophic microorganisms (Valentine et al., 2001). Methanotrophy is also of interest in a range of human-impacted contexts, including wastewater treatment plants (Ho et al., 2013), landfills (Scheutz et al., 2009), and oil spills (Crespo-Medina et al., 2014).

In addition to the climatic and economic implications of the methanotrophic process, its biochemical intricacies have stimulated many investigations. The anaerobic oxidation of methane (AOM) has proven particularly enigmatic, often involving a mutualistic relationship between anaerobic methanotrophic (ANME) archaea and sulfate reducing bacteria (SRB; Boetius et al., 2000). A consensus on the precise nature of the mutualism remains outstanding, but the net result of the process is typically the stoichiometric oxidation of methane coupled with sulfate reduction

Biogeosciences Discuss., doi:10.5194/bg-2016-202, 2016
Manuscript under review for journal Biogeosciences
Published: 19 May 2016

(Knittel and Boetius, 2009). Alternative electron acceptors including nitrate (Haroon et al., 2013), and nitrite (Ettwig et al., 2010) have been demonstrated, while several studies have presented equivocal evidence for methane oxidation coupled directly to iron or manganese reduction (Beal et al., 2009; Nauhaus et al., 2005; Sivan et al., 2014).

Methanotrophy is both a biogeochemically relevant reaction that modulates climate forcing and a biochemical curiosity; given this dual role, there is substantial interest in measuring the rate of the process and understanding elemental flows through metabolic pathways. AOM rate measurements have traditionally been conducted using a handful of techniques. Numerical models incorporating environmental sediment profiles of sulfate and methane concentrations can be used to back-calculate methane consumption rates (Jørgensen et al., 2001). Stable isotope $^{13}CH_4$ tracers can be used to probe longer-term rates in controlled conditions (Moran et al., 2008), but high levels of natural ^{13}C in marine dissolved inorganic carbon pools complicate the measurement (Pack et al., 2011). Gas chromatography quantification of dissolved (Girguis et al., 2003) or headspace (Carini et al., 2003) methane concentrations has also been demonstrated as a rate measurement tool, though low molarities make samples susceptible to exsolution if not processed quickly after collection, a requirement that may not be achievable in field settings. Perhaps the most sensitive approach uses radiolabeled $^{14}CH_4$ to track carbon movement into oxidized species (Alperin and Reeburgh, 1985; Treude et al., 2003). Tritiated methane was introduced for water column aerobic methane oxidation measurements due to its improved specific activity and the procedural advantages of working with a water-phase product rather than gaseous products (Valentine et al., 2001). Logistical and health and safety regulations led Pack et al. (2011) to develop an accelerator mass spectrometry detection method that requires 10^3-10^5 less radiolabel than previous ^{14}C and ^3H approaches, though the analytical procedure remains labor intensive.

Biogeosciences Discuss., doi:10.5194/bg-2016-202, 2016
Manuscript under review for journal Biogeosciences
Published: 19 May 2016

Despite the range of procedural options, methanotrophy rate measurements remain cumbersome, and the demonstration of a precise, safe, and easily enacted approach would be a welcome contribution for a diverse field of researchers. Nearly all of the aforementioned approaches are carbon-based; a hydrogen-based tracer offers an additional dimension to investigations of methane biochemical dynamics. Here we introduce a novel method for biologically mediated methanotrophy rate measurement that utilizes monodeuterated methane (CH_3D) as a substrate and measures the D/H ratio of the aqueous solution.

We demonstrate, through methanotrophic cell cultures and microcosm incubations of seafloor sediment and carbonate rock fragments, that aqueous D/H values are consistently proportional to ^{14}C-based rate measurements for given laboratory treatments tested in this study. The resulting ratios, when viewed in the context of partial versus complete methane oxidation, represent a new tool with which to examine the reversibility and catabolic / anabolic partitioning of methanotrophic metabolisms. As a rate measurement protocol, this approach offers several advantages over current techniques: it does not require the logistical, safety, and administrative hurdles associated with radiotracers such as $^{14}CH_4$ and ^{3}H-CH_4, it is less susceptible to analyte loss than methane headspace measurements, and compares favorably in terms of equipment cost and portability. The monodeuterated methane protocol offers new flexibility for practitioners and represents a useful and distinct new tool for the rate measurement of methanotrophic processes.

2. Methods

2.1. Experimental Set-Up

To demonstrate the precision and reproducibility of the monodeuterated methane approach, it was tested alongside the better-established $^{14}CH_4$ radiotracer protocol. Both techniques were

Biogeosciences Discuss., doi:10.5194/bg-2016-202, 2016
Manuscript under review for journal Biogeosciences
Published: 19 May 2016

applied to a) aerobic methanotrophic cultures of *Methylosinus trichosporium* and *Methyloprofundus sedimenti*, b) oxic incubations of methane seep sediment and carbonate rocks, and c) anoxic incubations of methane seep sediment and carbonate rocks. In addition, the monodeuterated methane protocol was employed on its own to demonstrate the relative effect of heightened, environmentally relevant pressure on methane consumption rates in anoxic seep sediment samples. Monodeuterated methane for all samples was 98% pure CH_3D obtained from Sigma-Aldrich ($247 / L). For a representation of all experiments conducted in this study, see Table 1.

2.1.1. Aerobic Methanotroph Cultures

Cultures of *Methylosinus trichosporium* strain OB3b (Whittenbury et al., 1970) were grown using Nitrate Mineral Salts (NMS) medium at 30 °C. The newly characterized *Methyloprofundus sedimenti* strain WF1 was grown in a modified NMS medium at 25 °C (Tavormina et al., 2015). In both cases, shaking cultures were grown up from stock in sealed 25 mL test tubes that contained 5 mL media and 50:50 air:methane by volume. After several successful transfers, experiments were initiated by passaging 0.94 mL of exponential phase inoculum into 8.5 mL media, for each of ten different experimental conditions, each prepared in triplicate (see Table S1). These conditions tested the CH_3D approach against killed, cell-free, oxygen-free, and CH_3D-free controls; parallel incubations incorporated $^{14}CH_4$ to allow for three time points of destructive sampling, and killed and radiolabel-free controls.

Samples for D/H analysis were taken at seven time points – most concentrated around anticipated exponential growth phases – throughout 140-hour (*M. trichosporium*) and 476-hour (*M. sedimenti*) experiments. Samples for radiolabel processing were taken at 46, 102, and 166.5

Biogeosciences Discuss., doi:10.5194/bg-2016-202, 2016
Manuscript under review for journal Biogeosciences
Published: 19 May 2016

hours for *M. trichosporium* cultures and 102, 166.5, and 432 hours for the slower-growing *M. sedimenti* cultures.

2.1.2. Environmental Samples: Methane Seep Sediments and Carbonates

Samples recovered from the Hydrate Ridge methane seep system were used to comparatively examine the novel monodeuterated methane (CH_3D) approach alongside the $^{14}CH_4$ protocol with environmental samples. Hydrate Ridge, Oregon, is located along a convergent tectonic margin and is well established as a site of methane seepage and sediment-based AOM (e.g., Suess et al., 1999; Treude et al., 2003; Tryon et al., 2002). Methane concentrations within the most active seep sediments reach several mM, and have been measured and modeled at values up to 70 mM (Boetius and Suess, 2004) and 50 mM (Tryon et al., 2002) respectively.

Samples used for methanotrophic rate experiments are specified in Table 1. All samples received a unique four-digit serial number. The "active" designation refers to sites where methane seepage was manifested by seafloor ecosystems known to be fueled by subsurface methane (e.g. clam beds and microbial mats) or methane bubble ebullition. The term "low activity" references sampling sites that did not exhibit any clear signs of contemporary methane seepage or chemosynthetic communities, though a small amount of methane supply and methanotrophic potential cannot be ruled out as subsurface advective flow can shift with time (Gieskes et al., 2005; Marlow et al., 2014; Tryon et al., 2002). The presence of carbonate pavements, coupled to depleted $\delta^{13}C_{carbonate}$ values suggest that they formed during "active" periods of seepage, consistent with previous descriptions (Naehr et al., 2007; Peckmann and Thiel, 2004). Sample types are abbreviated by the A.Sed (active sediment), A.Carb (active carbonate), L.Sed (low-activity sediment), and L.Carb (low-activity carbonate) designations. Seven samples were analyzed to examine a range of physical substrate type (sediment vs. carbonate rock) and seepage

Biogeosciences Discuss., doi:10.5194/bg-2016-202, 2016
Manuscript under review for journal Biogeosciences
Published: 19 May 2016

environments (active and low-activity): A.Sed-5128, A.Carb-5305, A.Carb-5152, L.Sed-5043, L.Carb-5028, and sterilized control aliquots of A.Sed-5128 and A.Carb-5305. Carbonate samples include both porous materials with macroscale vugs and pore spaces, as well as massive lithologies with more homogenous structure.

Samples were collected with the Deep Submergence Vehicle (DSV) *Alvin* during *Atlantis* leg AT-16-68 in September 2010 and the Remotely Operated Vehicle (ROV) *Jason* II during *Atlantis* leg AT-18-10 in September 2011. Shipboard, push cores and bottom water-submerged carbonates were immediately transferred to a 4 °C walk-in cold room and processed within several hours. To prepare material for future experimentation, compacted sediment and carbonate rocks were stored in anoxic, Ar-flushed mylar bags at 4 °C until use. In advance of experimental set-up, sediment and carbonate samples were prepared under anoxic conditions using 0.22 μm-filtered, anoxic N_2-sparged Hydrate Ridge bottom water (at a 1:2 sediment/carbonate:bottom water ratio by volume) and maintained under a $2x10^5$ Pa CH_4 headspace for one month.

To set up the experimental incubations, 10 mL physical substrate (compressed sediment or carbonate rock) and 20 mL filtered Hydrate Ridge bottom water were placed in 60-mL glass bottles (SVG-50 gaschro vials, Nichiden Riku Glass Co, Kobe, Japan). In all experiments involving carbonates, interior portions (> 5 cm from the rock surface) were used in order to ensure that properties exhibited were representative of bulk rock material and not a reflection of surface-based adherent cells or entrained material. Carbonate rock samples were fragmented in order to fit through the 28-mm diameter bottle opening; pieces were kept as large as possible to minimize the increase in surface area-to-volume ratio and maintain conditions as representative of the *in situ* environment as possible. All bottles were sealed with butyl stoppers; following several minutes of flushing with N_2 (g), the headspace was replaced with methane, and an additional 30 mL of gas

Biogeosciences Discuss., doi:10.5194/bg-2016-202, 2016
Manuscript under review for journal Biogeosciences
Published: 19 May 2016

was injected into the 30 mL headspace to generate the desired headspace composition at an absolute pressure of approximately $2x10^5$ Pa. Anoxic incubation headspace was 100% methane; oxic incubation headspace was 30 mL methane, 20 mL N_2, and 10 mL O_2. All incubation set-up prior to gas flushing and headspace injection took place in an anaerobic chamber. Triplicate samples, including killed controls, were prepared for all sample types. Measurements were taken for both D/H and ^{14}C analysis at 1.9 and 4 days for oxic incubations, and 3 and 8 days for anoxic incubations. Anoxic active methane seep sediment (A.Sed-5128) incubations were used for isotopic analysis of the remaining methane (set up in triplicate, with 60 mL CH_3D initial headspace) as well as empirical resolution studies sampled between days 20 and 22.

2.1.3. Pressurized samples

In order to probe the effect of pressure on anaerobic methanotrophic rates, a set of experiments was established, using the monodeuterated methane technique to determine relative rate differences. Active sediment from Hydrate Ridge (A.Sed-3450) was collected, processed shipboard, and prepared for experimentation as described above. To set up the incubations, eight 100 mL mylar bags were prepared with the components shown in Table S2: identical sets of four compositionally distinct samples were established such that each could be subjected to low and high pressure. Prior to gas addition, each bag was flushed for 5 minutes with Ar.

Once the incubations were prepared, they were transported to the laboratory of Dr. William Berelson at the University of Southern California and inserted into a stainless steel, custom-built pressure chamber with 3-cm thick walls and pressure valves rated to 40 MPa. The chamber was placed in a walk-in cold room (4 °C) on site, and hydraulic fluid was pumped into the sealed chamber using a Star Hydraulics P1A-250 hand pump. The pressure was maintained at 9.0 MPa (equivalent to ~900 m water depth) during the course of the 38-day experiment, with daily

Biogeosciences Discuss., doi:10.5194/bg-2016-202, 2016
Manuscript under review for journal Biogeosciences
Published: 19 May 2016

adjustments to account for thermal compression effects. At the conclusion of the experiment, mylar bags were removed from the chamber and checked for leaks (none were observed) and sampled for D/H ratio measurement.

2.2. Analytical Procedures

2.2.1. CH_3D Rate Measurements

At designated sampling times, ~1 mL of medium / water was collected from cultures or incubations in an anaerobic chamber with a sterile syringe. The liquid was then pushed through a 0.22 µm Durapore filter (EMD Millipore, Temecula, CA) and into a 1-mL GC vial. A LGR DLT-100 liquid water isotope analyzer (Los Gatos Research, Mountain View, CA) was used to determine the D/H ratio of each sample, with an injection volume of 700 nL at 1000 nL/s, four intra-injection flush strokes, and a flush time of 60 s between injections. Four rounds of ten injections per sample were performed in order to avoid memory effects; only the latter five injections were used in subsequent calculations. Sample runs were limited to ~250 injections in order to minimize salt precipitation, and each analysis included an appropriate blank (i.e., autoclaved media for the cultures, or filter sterilized bottom water used during incubation set-up in the case of sediment and carbonate incubations) and two standards of known isotopic ratios (Deep Blue: $\delta D = 0.5‰$, and CIT: $\delta D = -73.4‰$). Data was removed if instrumental temperature or pressure parameters were flagged as sub-optimal (0.76% of all analyses).

To calculate methane consumption rates, the number of deuterium atoms in the culture / incubation was calculated using the experiment's overall water volume and the adjusted D/H values (averaging across the latter five injections of the four distinct injection rounds). This value was multiplied by four given the 1:3 D:H stoichiometry of the CH_3D substrate to derive the number of methane molecules consumed through initial C-X bond activation. Known D/H ratios of

Biogeosciences Discuss., doi:10.5194/bg-2016-202, 2016
Manuscript under review for journal Biogeosciences
Published: 19 May 2016

the water standards were first used to generate a linear scaling factor that was applied to the corresponding data. To minimize instrumental drift, standards were re-measured between rounds of sample analysis (maximum of 40 injections) and new scaling factors were implemented. The scaling factor of four was used in the context of methane activation – the initial mobilization of the molecule through conversion to a methyl group – and is an end-member case that may not be appropriate for all subsequent processing as hydrogen/deuterium atoms are removed or exchanged. (Caveats and interpretation are discussed below, but consistent scaling factor implementation is the primary requirement for reliable comparison.) The resulting proxy value was divided by the incubation time and volume to arrive at a rate of methane consumption.

2.2.2. $^{14}CH_4$ Rate Measurements

Methane oxidation rates using radiolabeled methane substrate were measured as described in detail by Treude et al. (2005) and Treude and Ziebis (2010). Radiolabeled methane ($^{14}CH_4$ dissolved in seawater, corresponding to an activity of 13 kBq for culture experiments and 52 kBq in sediment and carbonate samples) was injected into each sample container, and samples were incubated at the appropriate temperatures for the designated amount of time (see above). To stop microbial activity and begin analysis, 2.5 ml of 2.5% NaOH was injected. Sample headspace was flowed through a Cu^{2+} oxide-filled 850 °C quartz tube furnace, combusting unreacted $^{14}CH_4$ to $^{14}CO_2$. This $^{14}CO_2$ was collected in two scintillation vials (23 ml volume) pre-filled with 7 ml phenylethylamine and 1 ml 2-methoxyethanol, to which 10 ml of scintillation cocktail (Ultima Gold XR, PerkinElmer) was added. After a 24-hour incubation period, radioactivity from $^{14}CO_2$ was measured by scintillation counting (Beckman Coulter LS 6500 Multi-Purpose Scintillation Counter, 10 minute analysis per sample).

Biogeosciences Discuss., doi:10.5194/bg-2016-202, 2016
Manuscript under review for journal Biogeosciences
Published: 19 May 2016

234 $^{14}CO_2$ and $H^{14}CO_3^-$ produced during the experimental period was quantified as follows.
235 The entire volume of each incubation sample was transferred into a 250-ml Erlenmeyer flask along
236 with 1 drop of antifoam and 5 ml of 6M HCl. The flask was immediately stoppered and sealed
237 with two clamps and parafilm wrapping to prevent gas escape, and placed on a shaking table (60
238 rpm, room temperature, 24 hours). To collect $^{14}CO_2$ generated by the acidification process, a 7-ml
239 scintillation vial was pre-filled with 1 ml of 2.5% NaOH and 1 ml of phenylethylamine and
240 suspended from the rubber stopper inside the flask. After the shaking / acidification step, 5 ml of
241 scintillation cocktail was added, and the vial was measured by scintillation counting after 24 hours.
242 This method has been demonstrated to recover 98% of $^{14}CO_2$ on average (Treude et al., 2003).
243 Finally, sterilized control samples (#10, see Table S2) were set aside after $^{14}CH_4$ addition
244 for gas chromatography to determine the initial concentration of methane gas. 400 µl of headspace
245 was injected into a gas chromatograph (Shimadzu GC-2014), equipped with a packed stainless
246 steel Supelco Custom Column (50/50 mixture, 80/100 Porapak N support, 80/100 Porapak Q
247 column, 6 ft x 1/8 in) and a flame ionization detector. The carrier gas was helium at a flow rate of
248 30 ml min^{-1}, and the column temperature was 60 °C. Results were scaled based on comparison
249 with standards of known methane concentrations (10 and 100 ppm; Matheson Tri-Gas, Twinsburg,
250 OH). The rate of methane oxidation was determined by the equation

251 $$Methane\ Oxidation = \frac{^{14}CO_2 \bullet CH_4}{(^{14}CH_4 + ^{14}CO_2) \bullet v \bullet t}$$

252 in which $^{14}CH_4$ is the combusted unreacted radiolabeled methane, $^{14}CO_2$ represents the quantity of
253 acidified oxidation product, CH_4 signifies the initial quantity of methane in the experiment, v is the
254 volume of sediment or carbonate rock, and t is the time over which the incubation was active.
255 *Isotopic Analysis of Methane in the Headspace*

Biogeosciences Discuss., doi:10.5194/bg-2016-202, 2016
Manuscript under review for journal Biogeosciences
Published: 19 May 2016

256 The methane headspace was analyzed via ^{1}H-NMR spectroscopy using a Varian 400 MHz
257 Spectrometer with a broadband auto-tune OneProbe. 300 µl of headspace was passed through
258 $CDCl_3$ with a fine needle to absorb the methane. ^{1}H-NMR spectra were acquired at 298 K without
259 spinning, using a repetition rate of 10 s to ensure reliable quantification. The spectra were
260 simulated with the iNMR 4.1.7 software for the determination of the fractional abundances of the
261 $^{12}CH_4$, $^{12}CH_3D$, $^{13}CH_4$ and $^{13}CH_3D$ isotopologs.
262
263 **3. Results and Discussion**
264 3.1. Aerobic Methanotroph Cultures
265 D/H ratios were acquired at eight points during the *M. trichosporium* growth curve and
266 seven points of the *M. sedimenti* growth curve; three measurements of ^{14}C distributions were
267 acquired for each strain, targeting exponential and stationary phases (Fig. 1). The Type II
268 alphaproteobacterial methanotroph *M. trichosporium* exhibited methane consumption rates more
269 than an order of magnitude greater than those of *M. sedimenti* (gammaproteobacterial Type I
270 methanotroph), yet the scaling factor relating the CH_3D- and $^{14}CH_4$-derived rates was remarkably
271 consistent in both cases. Using data points from both CH_3D and $^{14}CH_4$ experiments taken closest to
272 the end of exponential growth phase (47.5 hours for *M. trichosporium*, 140 and 102 hours for *M.*
273 *sedimenti* CH_3D and $^{14}CH_4$ measurements, respectively) and in stationary phase (140 and 166.5
274 hours for *M. trichosporium* CH_3D and $^{14}CH_4$ measurements; 476 and 432 hours for *M. sedimenti*
275 CH_3D and $^{14}CH_4$ measurements), the ratio of methane oxidation rates derived from each approach
276 can be compared. This value is hereafter referred to as the "H:C tracer ratio" because the CH_3D
277 method tracks hydrogen atoms, while the $^{14}CH_4$ approach traces carbon atoms (see "Understanding
278 the H:C Tracer Ratio", below). This ratio can be used to evaluate the consistency of the

Biogeosciences Discuss., doi:10.5194/bg-2016-202, 2016
Manuscript under review for journal Biogeosciences
Published: 19 May 2016

monodeuterated methane method compared with the better-established $^{14}CH_4$ approach, and as an investigatory tool in catabolic / anabolic processing of methane.

Using averaged values of tubes #1a, #1b, and #1c for CH_3D rates and the triplicate $^{14}CH_4$ tubes of the appropriate time point (#6, #7, or #8), H:C tracer ratio values were calculated and are shown in Table 2; their consistency is a promising indicator of the utility of the monodeuterated methane approach for ground-truthed rate measurements. By dividing rates derived from D/H values by 1.5, a reliable estimate of full-oxidation methanotrophy can be attained.

3.2. Environmental Samples: Methanotrophy Under Oxic and Anoxic Conditions

Oxidation rates under oxic microcosm incubation conditions, derived from both CH_3D and $^{14}CH_4$ measurements, are provided for all five sample types (active sediment, low-activity sediment, active porous carbonate, active massive carbonate, and low-activity massive carbonate) in Fig. 2a. The corresponding values for anoxic conditions are shown in Fig. 2b; all values were calculated from the second time point (4d for oxic conditions, 8d for anoxic conditions).

The H:C tracer ratio for the oxic incubations was 1.66 +/- 0.02 SE and 1.99 +/- 0.04 SE for anoxic conditions (Table 2). These relatively consistent values across physical substrate type (sediment and carbonates of varying lithology) and collection site activity level (active and low-activity) suggest an underlying metabolic basis of these H:C tracer ratios that is unperturbed by physicochemical factors or relative activity levels.

To determine the minimum number of activated CH_3D molecules needed for analytical detection, we assessed the length of time required to measure a differentiable D/H ratio. Measurements were acquired at multiple time points between days 20 and 22 of a triplicate set of A.Sed-5128 incubations. A resolvable signal of an enhanced D/H ratio was defined as data points with non-overlapping confidence intervals, representing a 95% statistical probability that D/H

Biogeosciences Discuss., doi:10.5194/bg-2016-202, 2016
Manuscript under review for journal Biogeosciences
Published: 19 May 2016

ratios were increased. Such differentiation seen at the 20-hour sampling time for two replicates and the 26-hour sampling time for the other one (Fig. S1). Using the rate determined by the first 20 days as a baseline, this translates to a resolution of 4.5-6.2 μmol of fully oxidized methane based on the H:C tracer ratio of 2.05 (Table 2).

3.3. Understanding the H:C Tracer Ratio

The CH_3D and $^{14}CH_4$ approaches quantify distinct aspects of methanotrophy, and each offers an important dimension in understanding methane metabolism. The $^{14}CH_4$ technique quantifies the amount of ^{14}C – initially supplied as methane – that is fully oxidized and persists as soluble species (HCO_3^-) or acid-labile precipitation products ($CaCO_3$). The CH_3D protocol, on the other hand, reports the extent to which methane-derived hydrogen atoms are found in the aqueous phase. Because methane is an inert molecule, D-H exchange of monodeuterated methane with water is negligible – an expectation borne out by the lack of significantly heightened D/H ratios in killed control experiments (e.g., Fig. 1). Its activation thereby indicates enzymatic functionalization, but the ultimate fate of each hydrogen during methane oxidation is unclear.

The flow of methane-derived hydrogen atoms through anaerobic and aerobic methanotrophic metabolisms was examined in an attempt to predictively evaluate the consequence of monodeuterated methane reactions. Previously published reports were used to compile Figure 3 (Hallam et al., 2004; Thauer, 2011; Vorholt and Thauer, 1997) and Figure 4 (Lieberman and Rosenzweig, 2004), which trace anaerobic and aerobic methane metabolisms, respectively, with a specific focus on hydrogen atoms. In this context, our observations of relatively consistent but distinct H:C tracer ratios for anaerobic and aerobic methanotrophy (Table 2) likely reflect different aspects of the two metabolic pathways. In AOM, metabolite backflux (Holler et al., 2011) may

Biogeosciences Discuss., doi:10.5194/bg-2016-202, 2016
Manuscript under review for journal Biogeosciences
Published: 19 May 2016

increase the D/H ratio; in aerobic methanotrophy, biomass growth represents a substantial carbon and hydrogen shunt.

3.3.1. The H:C Tracer Ratio in Anaerobic Methanotrophy

AOM is depicted via the reverse methanogenesis pathway in Fig. 3, whereby methyl-coenzyme M reductase (Mcr) activates methane and generates methyl-CoM. A tetrahydromethanopterin molecule supplants CoM, and subsequent carbon oxidation steps release hydrogen atoms into the medium. Ultimately, the number of methane-derived hydrogen atoms that enter water-exchangeable products dictates the physiological interpretation of waterborne D/H ratios. For example, if just one methane-derived hydrogen enters an intermediate and is freely exchangeable with water, then observed water-based deuterium must be multiplied by four (to account for methane's hydrogen-carbon stoichiometry) and a primary isotope effect as high as 2.44 (*M. marburgensis'* Mcr's C-H vs. C-D bond-breaking preference, Scheller et al., 2013) to arrive at the actual quantity of activated methane molecules. In this context, the experimental H:C tracer ratio values may provide useful insight. A H:C tracer ratio of 2 for the reverse methanogenesis pathway suggests that, for every methane molecule that is fully oxidized to CO_2, two hydrogen atoms enter water-exchangeable intermediates.

However, heightened D/H ratios may occur in the absence of full carbon oxidation and could be partially attributable to the back reaction of enzymatic processes (Scheller et al., 2010) involving hydrogen exchange with the aqueous medium. For example, upon the activation of methane by Mcr, HS-CoB and CH_3-S-CoM form, with the thiol hydrogen exchanging with water-bound hydrogen. If the S-bound hydrogen were deuterium, then the re-formation of methane (CH_4) would result in a heightened aqueous D/H ratio but no net methane consumption (Fig. 3). We analyzed the remaining headspace for the formation of CH_4 from CH_3D via ^{1}H-NMR

Biogeosciences Discuss., doi:10.5194/bg-2016-202, 2016
Manuscript under review for journal Biogeosciences
Published: 19 May 2016

spectroscopy. Over the course of 58 days in triplicate seep sediment incubations prepared with exclusively CH_3D headspace, CH_4 in the headspace increased from 0.33% +/- 0.02% SE to 4.48% +/- 0.27% SE. If this demonstrated reversibility only reflects the back reaction of Mcr, then the CH_4 increase must be multiplied by four to reflect the actual percentage of headspace methane that was re-formed by Mcr; if the reversibility reflects back reaction of the entire pathway, then no scaling factor is needed. Thus, the range of potential methane headspace percentage accounted for by methane reformed from initial CH_3D is between 4.15 – 16.6%. For clarity, these calculations neglect isotope effects and activity by methanogens, factors that can be clarified through further experimentation. For example, reversibility can be evaluated by a) including a ^{13}C-dissolved inorganic carbon (DIC) signal in the water and measuring $^{13}CH_4$, and/or b) utilizing multiply deuterated methane as initial headspace and quantifying all possible isotopologs. Nonetheless, even the upper bound of partially and reversibly oxidized CH_3D suggests that the majority of the D/H signal is attributable to reactions indicative of net methane consumption, if not complete oxidation.

3.3.2. The H:C Tracer Ratio in Aerobic Methanotrophy

In aerobic methanotrophic cultures, a H:C tracer ratio of ~1.5 was observed, suggesting that on average, 2.67 of the four methane-derived hydrogen atoms likely enter water-exchangeable products during the course of a full oxidation pathway. Intriguingly, this ratio was similar for both cultured organisms despite their distinct metabolic pathways. *M. tricosporium* is a type II methanotroph, a member of the *Alphaproteobacteria* that uses the serine pathway for carbon assimilation *M. sedimenti* is a gammaproteobacterial type I methanotroph, using the ribulose monophosphate (RuMP) carbon assimilation pathway (Tavormina et al., 2015). The pathway data presented in Fig. 4 suggests that all methane-bound hydrogens are water exchangeable during the catabolic oxidation of methane to carbon dioxide. Thus, to achieve a H:C tracer ratio less than 4, a

Biogeosciences Discuss., doi:10.5194/bg-2016-202, 2016
Manuscript under review for journal Biogeosciences
Published: 19 May 2016

substantial proportion of methane-derived formaldehyde would need to proceed down the assimilatory pathway, a requirement that was likely met given the cultures' increase in cell density.

The oxic incubations of methane seep sediment produced a H:C tracer ratio of 1.66 +/- 0.02 SE. Given that the known modes of biological methane oxidation – type I and type II aerobic methanotrophy and reverse methanogenesis anaerobic methanotrophy – bound this observed value, it appears likely that the oxic sediment incubations supported a mixture of both aerobic and anaerobic methane oxidation processes. Aerobic methane oxidation likely dominated, based on the ~$7x10^4$ Pa partial pressure of O_2 and the proximity of the H:C tracer ratio to that of the aerobic methanotrophic cultures, but anoxic niches likely remained or developed in the incubation bottles.

3.4. Validating the Monodeuterated Methane Approach: Anaerobic Methanotrophy at Pressure

To demonstrate the utility of the CH_3D rate measurement approach in addressing experimentally relevant questions, we sought to evaluate the influence of *in situ* pressure on methanotrophic rates of Hydrate Ridge seep sediment microbial communities. Material collected for microbiological studies of AOM is frequently obtained from marine settings of various depths that are subjected to distinct and substantial pressure regimes (Ruff et al., 2015). Pressure is not always rigorously incorporated into microcosm experiments, though evidence suggests it can be an important determinant of methanotrophic rates (Bowles et al., 2011; Nauhaus et al., 2005; Zhang et al., 2010).

Parallel seep sediment incubations were subjected to 0.1 MPa (atmospheric pressure) and 9.0 MPa (equivalent to ~900 m depth). Measured rates, expressed in δD values derived from D/H ratios, are shown in Fig. 5. A significant increase in methane consumption was observed in both live conditions at heightened pressure, corresponding to sediment incubated with isotopically labeled glycine (samples 1a and 1b) and ammonium chloride (samples 2a and 2b). Controls

Biogeosciences Discuss., doi:10.5194/bg-2016-202, 2016
Manuscript under review for journal Biogeosciences
Published: 19 May 2016

393 lacking CH_3D (samples 3a and 3b) and biological activity (samples 4a and 4b) showed no increase
394 in D/H ratios (see Table S2 for sample set-up details). The simulation of *in situ* Hydrate Ridge
395 pressures led to a 79.5% (+/- 6.5 SE) increase in relative methane oxidizing rates. Incubation with
396 500 μM glycine rather than ammonia at high and low pressures resulted in small but consistent rate
397 increases of 12% +/- 4.1% SE, potentially reflecting the energetic and biosynthetic distinction
398 between exogenous amino acids and unprocessed fixed nitrogen.

399 Previous reports have found a wide range of different pressure-related effects. In a sulfate-
400 coupled AOM bioreactor, pressures were varied from 1 to 8 MPa and sulfide production
401 approximately tripled, demonstrating Michaelis-Menten style kinetics with an apparent K_m of 37
402 mM (Zhang et al., 2010). Methane partial pressures of 1.1 MPa led to a 5x increase in sulfate
403 reduction rates relative to ambient atmospheric pressure with Hydrate Ridge sediments
404 demonstrating methane-dependent sulfate reduction (Nauhaus et al., 2002). With methane seep
405 sediment from the Japan Trench, however, methane-driven sulfate reduction rates did not correlate
406 with changing pressure (Vossmeyer et al., 2012). Nauhaus et al. (2005) suggested that the pressure-
407 induced rate increases are due more to heightened methane solubility and bioavailability rather
408 than physiological effects or biomolecular re-ordering. Bowles et al. (2011) presented a very
409 different perspective by showing a six- to ten-fold AOM rate increase at 10 MPa when methane
410 concentrations were held constant. Deconvolving these two influences and how they depend on
411 community composition or physicochemical parameters is feasible with pressure chamber
412 experiments utilizing monodeuterated methane. Understanding the relative contributions of
413 environmental and physiological effects to methane oxidation will help constrain methane fluxes
414 across a larger envelope of the planet's methanotrophically active zones.

415 3.5. Monodeuterated Methane in Experimental Investigations

Biogeosciences Discuss., doi:10.5194/bg-2016-202, 2016
Manuscript under review for journal Biogeosciences
Published: 19 May 2016

Based on $^{14}CH_4$ ground-truthing experiments with aerobic methanotrophic cultures, oxic seep sediment, and anoxic seep sediment, as well as the proof-of-concept pressurized experiments, we believe that the monodeuterated methane approach to methane oxidation rate measurement is a useful addition to the biogeochemist's tool set. Compared with radiolabel approaches ($^{14}CH_4$, ^{3}H-CH_4, $^{35}SO_4^{2-}$), the method requires less safety-oriented planning, and is logistically simpler, more affordable, and less susceptible to isotope fractionation effects. Our results suggest that it appears to be a more precise method based on standard error calculations, though direct comparisons are complicated by the fact that different aliquots of the same initial material were used. Because the monodeuterated methane method focuses on methane-bound hydrogen atoms, it offers different, complementary information about methanotrophic systems than carbon-based techniques like methane or bicarbonate quantification. While this distinction complicates the interpretation of isolated D/H ratios, it can offer an additional dimension of information for analysis of methane-derived intermediates in relevant metabolisms. Given these caveats, we recommend three use cases for monodeuterated methane in methane oxidation rate measurement applications.

1) First, the approach can be employed in a strictly comparative context using analogous inoculum exposed to a range of different conditions, as demonstrated with the pressure-based sediment incubations presented above. Evaluating the effect of different conditions such as temperature ranges, chemical concentrations, or energetic landscapes on seep sediment methane oxidizing rates would all be promising applications. Comparative analysis of AOM rates at different seep sites would also be useful, provided anaerobic or aerobic methanotrophic processes could be isolated.

2) Second, by performing side-by-side monodeuterated methane and radiocarbon tests, a sample-specific H:C tracer ratio can be determined, and absolute rates of full methane

Biogeosciences Discuss., doi:10.5194/bg-2016-202, 2016
Manuscript under review for journal Biogeosciences
Published: 19 May 2016

oxidation can then be inferred in subsequent experiments based exclusively on D/H ratios. Conducting such paired studies under additional environmental or lab-based conditions would help clarify the universality of the ratios presented here and would likely reveal additional questions of metabolic dynamics in a range of experimental systems.

3) Finally, the use of monodeuterated methane as an analytical tool, alongside additional methods such as carbon- or sulfur-tracking procedures, would enable a multi-dimensional examination of anabolic and catabolic processes in methane-based metabolisms. In particular, the H:C tracer ratios presented here reveal intriguing and seemingly systematic relationships between carbon and hydrogen anabolic and catabolic partitioning across distinct physiologies, yet an underlying theoretical framework regarding the fate of methane-bound hydrogen atoms remains outstanding. In anaerobic methanotrophic systems, back-reaction rates and equilibrium constants could be evaluated by a) including a $^{13}CO_2$ signal in the water and measuring $^{13}CH_4$, and/or b) utilizing multiply deuterated methane as initial headspace and measuring all possible isotopologues via nuclear magnetic resonance (NMR) or high resolution mass spectrometry. For aerobic methanotrophs, evaluating H:C tracer ratios under more clearly defined growth and maintenance phases would elucidate distinct H:C tracer ratios associated with catabolic, RuMP, and serine pathways, enabling future use of that parameter as an arbiter of relative anabolic and catabolic activity. Furthermore, additional environmental variables can be tested to gain insight into distinct redox pathways and dynamics of reversibility. For example, AOM under lower sulfate concentrations might be expected to generate higher H:C tracer ratios (Yoshinaga et al.,

Biogeosciences Discuss., doi:10.5194/bg-2016-202, 2016
Manuscript under review for journal Biogeosciences
Published: 19 May 2016

462 2014), and this parameter could be further developed as a measure of microbially
463 mediated isotopic equilibration.
464
465 **4. Conclusion**
466 The ability to accurately measure methane oxidation rates – both comparatively and in
467 absolute values – is an important component of methanotrophic studies. Such measurements
468 frequently depend on radiotracers or measurements of chemical species that are related to, but not
469 directly indicative of, methane metabolism. The monodeuterated methane technique presented here
470 represents a novel approach to methane oxidation rate measurements, notable for its logistical and
471 analytical ease (particularly in ship-board applications), as well as the added dimension provided
472 by H-based, rather than C-based, information. We have demonstrated that the D/H ratio is directly
473 proportional to methane oxidation rates as measured in absolute terms by the well-established
474 $^{14}CH_4$ method. The value of the proportionality constant differs based on the experimental system,
475 likely dictated by relative proportions of aerobic and anaerobic methanotrophic metabolisms,
476 though additional experiments to determine the nature of the putative mixing line are needed.
477 Methane biogeochemistry is a dynamic field of study with implications for carbon cycling,
478 microbial ecology, and climate dynamics, though experimental challenges have slowed our
479 understanding of methane-based biological reactions. With the CH_3D approach as an added tool in
480 the arsenal of rate-based examinations, a broader understanding of the intricacies of methane
481 metabolism, as well as its role in environmental and anthropogenic systems, is within reach.
482
483 **5. Acknowledgements**

Biogeosciences Discuss., doi:10.5194/bg-2016-202, 2016
Manuscript under review for journal Biogeosciences
Published: 19 May 2016

We thank the Captains, Crew, *Alvin* group, *Jason* group, and Science party members from *RV Atlantis* legs AT-15-68, and AT-18-10. Water analyzer measurements were conducted in the laboratory of Alex Sessions at the California Institute of Technology with technical support from Lichun Zhang. We are indebted to William Berelson at the University of Southern California and Nick Rollins for use of their pressure chambers and assistance with the incubation experiments. We thank Alex Sessions, Woodward Fischer, Dianne Newman, Tori Hoehler, Amy Rosenzweig, and Daniel Stolper for helpful conversations during the preparation of the manuscript. This study was funded by grants from the U.S. Department of Energy, Office of Science, Office of Biological and Environmental Research (DE-SC001057), the NASA Astrobiology Institute (Award # NNA13AA92A) and support from the Gordon and Betty Moore Foundation through grant GBMF3780 (to VJO). JJM was supported by a National Energy Technology Laboratory Methane Hydrate Research Fellowship funded by the National Research Council of the National Academies. This research used resources of the Oak Ridge Leadership Computing Facility. Oak Ridge National Laboratory is supported by the Office of Science of the U.S. Department of Energy.

6. References

Alperin, M. J., and Reeburgh, W. S. (1985). Inhibition Experiments on Anaerobic Methane Oxidation. *Applied and Environmental Microbiology* 50, 940–945.

Beal, E. J., House, C. H., and Orphan, V. J. (2009). Manganese- and Iron-Dependent Marine Methane Oxidation. *Science* 325, 184–187. doi:10.1126/science.1169984.

Boetius, A., Ravenschlag, K., Schubert, C. J., Rickert, D., Widdel, F., Gleseke, A., et al. (2000). A marine microbial consortium apparently mediating anaerobic oxidation of methane. *Nature* 407.

Boetius, A., and Suess, E. (2004). Hydrate Ridge: a natural laboratory for the study of microbial life fueled by methane from near-surface gas hydrates. *Chemical Geology* 205, 291–310. doi:10.1016/j.chemgeo.2003.12.034.

510 Bowles, M. W., Samarkin, V. A., and Joye, S. B. (2011). Improved measurement of microbial
511 activity in deep-sea sediments at in situ pressure and methane concentration. *Limnology*
512 *and Oceanography: Methods* 9, 499–506.

513 Carini, S. A., Orcutt, B. N., and Joye, S. B. (2003). Interactions between methane oxidation and
514 nitrification in coastal sediments. *Geomicrobiology Journal* 20, 355–374.

515 Crespo-Medina, M., Meile, C., Hunter, K., Diercks, A., Asper, V., Orphan, V., et al. (2014). The
516 rise and fall of methanotrophy following a deepwater oil-well blowout. *Nature Geoscience*.

517 Ettwig, K. F., Butler, M. K., Le Paslier, D., Pelletier, E., Mangenot, S., Kuypers, M. M., et al.
518 (2010). Nitrite-driven anaerobic methane oxidation by oxygenic bacteria. *Nature* 464, 543–
519 548.

520 Gieskes, J., Mahn, C., Day, S., Martin, J. B., Greinert, J., Rathburn, T., et al. (2005). A study of the
521 chemistry of pore fluids and authigenic carbonates in methane seep environments: Kodiak
522 Trench, Hydrate Ridge, Monterey Bay, and Eel River Basin. *Chemical Geology* 220, 329–
523 345. doi:10.1016/j.chemgeo.2005.04.002.

524 Girguis, P. R., Orphan, V. J., Hallam, S. J., and DeLong, E. F. (2003). Growth and Methane
525 Oxidation Rates of Anaerobic Methanotrophic Archaea in a Continuous-Flow Bioreactor.
526 *Applied and Environmental Microbiology* 69, 5472–5482. doi:10.1128/AEM.69.9.5472-
527 5482.2003.

528 Hallam, S. J., Putnam, N., Preston, C. M., Detter, J. C., Rokhsar, D., Richardson, P. M., et al.
529 (2004). Reverse methanogenesis: testing the hypothesis with environmental genomics.
530 *Science* 305, 1457–1462.

531 Haroon, M. F., Hu, S., Shi, Y., Imelfort, M., Keller, J., Hugenholtz, P., et al. (2013). Anaerobic
532 oxidation of methane coupled to nitrate reduction in a novel archaeal lineage. *Nature* 500,
533 567–570.

534 Ho, A., Vlaeminck, S. E., Ettwig, K. F., Schneider, B., Frenzel, P., and Boon, N. (2013). Revisiting
535 methanotrophic communities in sewage treatment plants. *Applied and environmental*
536 *microbiology* 79, 2841–2846.

537 Holler, T., Wegener, G., Niemann, H., Deusner, C., Ferdelman, T. G., Boetius, A., et al. (2011).
538 Carbon and sulfur back flux during anaerobic microbial oxidation of methane and coupled
539 sulfate reduction. *Proceedings of the National Academy of Sciences* 108, E1484–E1490.
540 doi:10.1073/pnas.1106032108.

541 Holzapfel-Pschorn, A., Conrad, R., and Seiler, W. (1985). Production, oxidation and emission of
542 methane in rice paddies. *FEMS Microbiology Ecology* 1, 343–351.

543 Jørgensen, B. B., Weber, A., and Zopfi, J. (2001). Sulfate reduction and anaerobic methane
544 oxidation in Black Sea sediments. *Deep Sea Research Part I: Oceanographic Research*
545 *Papers* 48, 2097–2120.

Biogeosciences Discuss., doi:10.5194/bg-2016-202, 2016
Manuscript under review for journal Biogeosciences
Published: 19 May 2016

546 Knittel, K., and Boetius, A. (2009). Anaerobic Oxidation of Methane: Progress with an Unknown
547 Process. *Annu. Rev. Microbiol.* 63, 311–334.
548 doi:10.1146/annurev.micro.61.080706.093130.

549 Lieberman, R. L., and Rosenzweig, A. C. (2004). Biological methane oxidation: regulation,
550 biochemistry, and active site structure of particulate methane monooxygenase. *Critical*
551 *reviews in biochemistry and molecular biology* 39, 147–164.

552 Mackelprang, R., Waldrop, M. P., DeAngelis, K. M., David, M. M., Chavarria, K. L., Blazewicz,
553 S. J., et al. (2011). Metagenomic analysis of a permafrost microbial community reveals a
554 rapid response to thaw. *Nature* 480, 368–371.

555 Marlow, J. J., Steele, J. A., Ziebis, W., Thurber, A. R., Levin, L. A., and Orphan, V. J. (2014).
556 Carbonate-hosted methanotrophy represents an unrecognized methane sink in the deep sea.
557 *Nature Communications*.

558 Mason, O., Case, D., Naehr, T., Lee, R., Thomas, R., Bailey, J., et al. (2015). Comparison of
559 Archaeal and Bacterial Diversity in Methane Seep Carbonate Nodules and Host Sediments,
560 Eel River Basin and Hydrate Ridge, USA. *Microb Ecol* 70, 766–784. doi:10.1007/s00248-
561 015-0615-6.

562 Moran, J. J., Beal, E. J., Vrentas, J. M., Orphan, V. J., Freeman, K. H., and House, C. H. (2008).
563 Methyl sulfides as intermediates in the anaerobic oxidation of methane. *Environmental*
564 *Microbiology* 10, 162–173. doi:10.1111/j.1462-2920.2007.01441.x.

565 Naehr, T. H., Eichhubl, P., Orphan, V. J., Hovland, M., Paull, C. K., Ussler III, W., et al. (2007).
566 Authigenic carbonate formation at hydrocarbon seeps in continental margin sediments: A
567 comparative study. *Deep Sea Research Part II: Topical Studies in Oceanography* 54,
568 1268–1291. doi:10.1016/j.dsr2.2007.04.010.

569 Nauhaus, K., Boetius, A., Krüger, M., and Widdel, F. (2002). In vitro demonstration of anaerobic
570 oxidation of methane coupled to sulphate reduction in sediment from a marine gas hydrate
571 area. *Environmental Microbiology* 4, 296–305. doi:10.1046/j.1462-2920.2002.00299.x.

572 Nauhaus, K., Treude, T., Boetius, A., and Krüger, M. (2005). Environmental regulation of the
573 anaerobic oxidation of methane: a comparison of ANME-I and ANME-II communities.
574 *Environmental Microbiology* 7, 98–106. doi:10.1111/j.1462-2920.2004.00669.x.

575 Orphan, V. J., Ussler III, W., Naehr, T. ., House, C. ., Hinrichs, K.-U., and Paull, C. . (2004).
576 Geological, geochemical, and microbiological heterogeneity of the seafloor around
577 methane vents in the Eel River Basin, offshore California. *Chemical Geology* 205, 265–
578 289. doi:10.1016/j.chemgeo.2003.12.035.

579 Pack, M. A., Heintz, M. B., Reeburgh, W. S., Trumbore, S. E., Valentine, D. L., Xu, X., et al.
580 (2011). A method for measuring methane oxidation rates using lowlevels of 14C‐labeled
581 methane and accelerator mass spectrometry. *Limnology and Oceanography: Methods* 9,
582 245–260.

Biogeosciences Discuss., doi:10.5194/bg-2016-202, 2016
Manuscript under review for journal Biogeosciences
Published: 19 May 2016

583 Peckmann, J., and Thiel, V. (2004). Carbon cycling at ancient methane–seeps. *Chemical Geology*
584 205, 443–467. doi:10.1016/j.chemgeo.2003.12.025.

585 Reeburgh, W. S. (2007). Oceanic Methane Biogeochemistry. *Chem. Rev.* 107, 486–513.
586 doi:10.1021/cr050362v.

587 Ruff, S. E., Biddle, J. F., Teske, A. P., Knittel, K., Boetius, A., and Ramette, A. (2015). Global
588 dispersion and local diversification of the methane seep microbiome. *Proceedings of the*
589 *National Academy of Sciences*, 201421865.

590 Scheller, S., Goenrich, M., Boecher, R., Thauer, R. K., and Jaun, B. (2010). The key nickel
591 enzyme of methanogenesis catalyses the anaerobic oxidation of methane. *Nature* 465, 606–
592 608.

593 Scheller, S., Goenrich, M., Thauer, R. K., and Jaun, B. (2013). Methyl-Coenzyme M Reductase
594 from Methanogenic Archaea: Isotope Effects on the Formation and Anaerobic Oxidation of
595 Methane. *J. Am. Chem. Soc.* 135, 14975–14984. doi:10.1021/ja406485z.

596 Scheutz, C., Bogner, J., De Visscher, A., Gebert, J., Hilger, H., Huber-Humer, M., et al. (2009).
597 Microbial methane oxidation processes and technologies for mitigation of landfill gas
598 emissions. *Waste Management & Research*.

599 Sivan, O., Antler, G., Turchyn, A. V., Marlow, J. J., and Orphan, V. J. (2014). Iron oxides
600 stimulate sulfate-driven anaerobic methane oxidation in seeps. *Proceedings of the National*
601 *Academy of Sciences* 111, E4139–E4147. doi:10.1073/pnas.1412269111.

602 Suess, E., Torres, M., Bohrmann, G., Collier, R., Greinert, J., Linke, P., et al. (1999). Gas hydrate
603 destabilization: enhanced dewatering, benthic material turnover and large methane plumes
604 at the Cascadia convergent margin. *Earth and Planetary Science Letters* 170, 1–15.

605 Tavormina, P. L., Hatzenpichler, R., McGlynn, S., Chadwick, G., Dawson, K. S., Connon, S. A., et
606 al. (2015). Methyloprofundus sedimenti gen. nov., sp. nov., an obligate methanotroph from
607 ocean sediment belonging to the "deep sea-1"clade of marine methanotrophs. *International*
608 *journal of systematic and evolutionary microbiology* 65, 251–259.

609 Thauer, R. K. (2011). Anaerobic oxidation of methane with sulfate: on the reversibility of the
610 reactions that are catalyzed by enzymes also involved in methanogenesis from CO 2.
611 *Current opinion in microbiology* 14, 292–299.

612 Treude, Boetius, Knittel, Wallmann, and Jorgensen (2003). Anaerobic oxidation of methane above
613 gas hydrates at Hydrate Ridge, NE Pacific Ocean. *Mar Ecol Prog Ser* 264, 1–14.

614 Treude, T., Krüger, M., Boetius, A., and Jørgensen, B. B. (2005). Environmental control on
615 anaerobic oxidation of methane in the gassy sediments of Eckernfoerde Bay(German
616 Baltic). *Limnology and oceanography* 50, 1771–1786.

617 Treude, T., and Ziebis, W. (2010). Methane oxidation in permeable sediments at hydrocarbon
618 seeps in the Santa Barbara Channel, California. *Biogeosciences (BG)* 7, 3095–3108.

Tryon, M. ., Brown, K. ., and Torres, M. . (2002). Fluid and chemical flux in and out of sediments hosting methane hydrate deposits on Hydrate Ridge, OR, II: Hydrological processes. *Earth and Planetary Science Letters* 201, 541–557. doi:10.1016/S0012-821X(02)00732-X.

Valentine, D. L., Blanton, D. C., Reeburgh, W. S., and Kastner, M. (2001). Water column methane oxidation adjacent to an area of active hydrate dissociation, Eel river Basin. *Geochimica et Cosmochimica Acta* 65, 2633–2640. doi:10.1016/S0016-7037(01)00625-1.

Vorholt, J. A., and Thauer, R. K. (1997). The Active Species of "CO2" Utilized by Formylmethanofuran Dehydrogenase from Methanogenic Archaea. *European Journal of Biochemistry* 248, 919–924. doi:10.1111/j.1432-1033.1997.00919.x.

Vossmeyer, A., Deusner, C., Kato, C., Inagaki, F., and Ferdelman, T. G. (2012). Substrate-specific pressure-dependence of microbial sulfate reduction in deep-sea cold seep sediments of the Japan Trench. *Frontiers in Microbiology* 3, 253. doi:10.3389/fmicb.2012.00253.

Whittenbury, R., Phillips, K., and Wilkinson, J. (1970). Enrichment, isolation and some properties of methane-utilizing bacteria. *Journal of General Microbiology* 61, 205–218.

Yoshinaga, M. Y., Holler, T., Goldhammer, T., Wegener, G., Pohlman, J. W., Brunner, B., et al. (2014). Carbon isotope equilibration during sulphate-limited anaerobic oxidation of methane. *Nature Geosci* 7, 190–194.

Zhang, Y., Henriet, J.-P., Bursens, J., and Boon, N. (2010). Stimulation of in vitro anaerobic oxidation of methane rate in a continuous high-pressure bioreactor. *Bioresource Technology* 101, 3132–3138. doi:10.1016/j.biortech.2009.11.103.

7. Tables and Figure Captions

Table 1: A summary of the samples used for all experiments conducted in this study. Green boxes indicate that the experiment took place (with all relevant permutations and controls, as described in the text); blank boxes indicate experiments that were not conducted. CH_3D refers to methanotrophic rate experiments using the novel monodeuterated methane technique, while $^{14}CH_4$ refers to the radiolabel-based experiments. The three-part codes for samples derived from environmental material refer to active (A) or low-activity (L) sediments (Sed) or carbonates (Carb), as explained in the text.

Biogeosciences Discuss., doi:10.5194/bg-2016-202, 2016
Manuscript under review for journal Biogeosciences
Published: 19 May 2016

650

		Oxic		Anoxic	
		CH_3D	$^{14}CH_4$	CH_3D	$^{14}CH_4$
Aerobic Methanotroph Cultures Experiment					
	M. trichosporium				
	M. sedimenti				
Seep Sediment Experiment					
	A.Sed-5128				
	L.Sed-5043				
Seep Carbonate Experiment					
	A.Carb-5305				
	A.Carb-5152				
	L.Carb-5028				
Pressure Experiment					
	A.Sed-3450				

651
652

653 Table 2: H:C tracer ratios for the experimental treatments addressed in this study.

654

Aerobic Methanotroph Cultures		
	Exponential Phase	Stationary Phase
M. trichosporium	1.5	1.48
M. sedimenti	1.54	1.59
Methane Seep Sediments and Carbonates		
	Oxic Incubations	Anoxic Incubations
A.Sed-5128	1.62	2.05
L.Sed-5043	1.71	2.01
A.Carb-5305	1.65	1.96
A.Carb-5152	1.63	2.08
L.Carb-5028	1.69	1.86

655

656

657 Fig. 1: Amount of methane oxidized over time for cultures of a) the type II methanotroph *M.*
658 *trichosporium* and b) the type I methanotroph *M. sedimenti* using the CH_3D method (circles) and
659 the $^{14}CH_4$ method (diamonds), calculated as discussed in the text. Symbols correspond to sample
660 types as follows: blue = CH_3D-derived experimental data; brown = CH_3D killed control data;
661 orange = CH_3D abiotic control data; gray = CH_3D oxygen-free, argon-infused control data; green =
662 CH_4 control data; red = $^{14}CH_4$ –derived experimental data; black = $^{14}CH_4$ –derived killed control

Biogeosciences Discuss., doi:10.5194/bg-2016-202, 2016
Manuscript under review for journal Biogeosciences
Published: 19 May 2016

663 data. Error bars show standard errors for three biological replicates, with the exception of the $^{14}CH_4$
664 –derived killed control (n=1). Data obscured by other data series exhibited values between -60 and
665 110 nmol for a) and 0 and 60 nmol for b).
666
667 Fig. 2: Methane oxidation rates of a) oxic and b) anoxic incubations of active and inactive seep
668 sediment and carbonate rocks (n=3 in all cases). Values compare rates derived from the $^{14}CH_4$
669 (blue) and CH_3D (green) experiments for a given sample material; standard error bars provided.
670
671 Fig. 3: A schematic diagram demonstrating the potential fate of methane-associated hydrogen
672 atoms in the "reverse methanogenesis" pathway. Hydrogen atoms are distinguished by color and
673 superscript number, and potential exchanges with inter- and intra-cellular water are shown.
674 Potentially detectable methane-derived hydrogen atoms (4, occurring throughout the oxidation
675 pathway) and carbon atoms (1, requiring full oxidation) are highlighted in orange and purple
676 boxes, respectively. Arrows are unidirectional to demonstrate the net methane-consuming direction
677 of the pathway, but all enzymes have been shown to be reversible (Thauer, 2008), a situation that is
678 shown explicitly only for Mcr. The extended dashed line represents the cell membrane.
679
680 Fig. 4: A schematic diagram demonstrating the potential fate of methane-associated hydrogen
681 atoms in the aerobic methanotrophy pathways. Hydrogen atoms are distinguished by color and
682 superscript number; asterisks represent location-specific ambiguity. Potentially detectable
683 methane-derived hydrogen atoms and carbon atoms are highlighted in orange and purple boxes,
684 respectively. Mmo enzymes are not believed to perform reversible reactions.
685

Biogeosciences Discuss., doi:10.5194/bg-2016-202, 2016
Manuscript under review for journal Biogeosciences
Published: 19 May 2016

686 Fig. 5: Water δD values with standard error bars of seep sediment samples following 38-day

687 incubations with CH_3D at 9.0 MPa (brown bars, "b" samples) or 0.1 MPa (pink bars, "a" samples).

Biogeosciences Discuss., doi:10.5194/bg-2016-202, 2016
Manuscript under review for journal Biogeosciences
Published: 19 May 2016

Figure 1

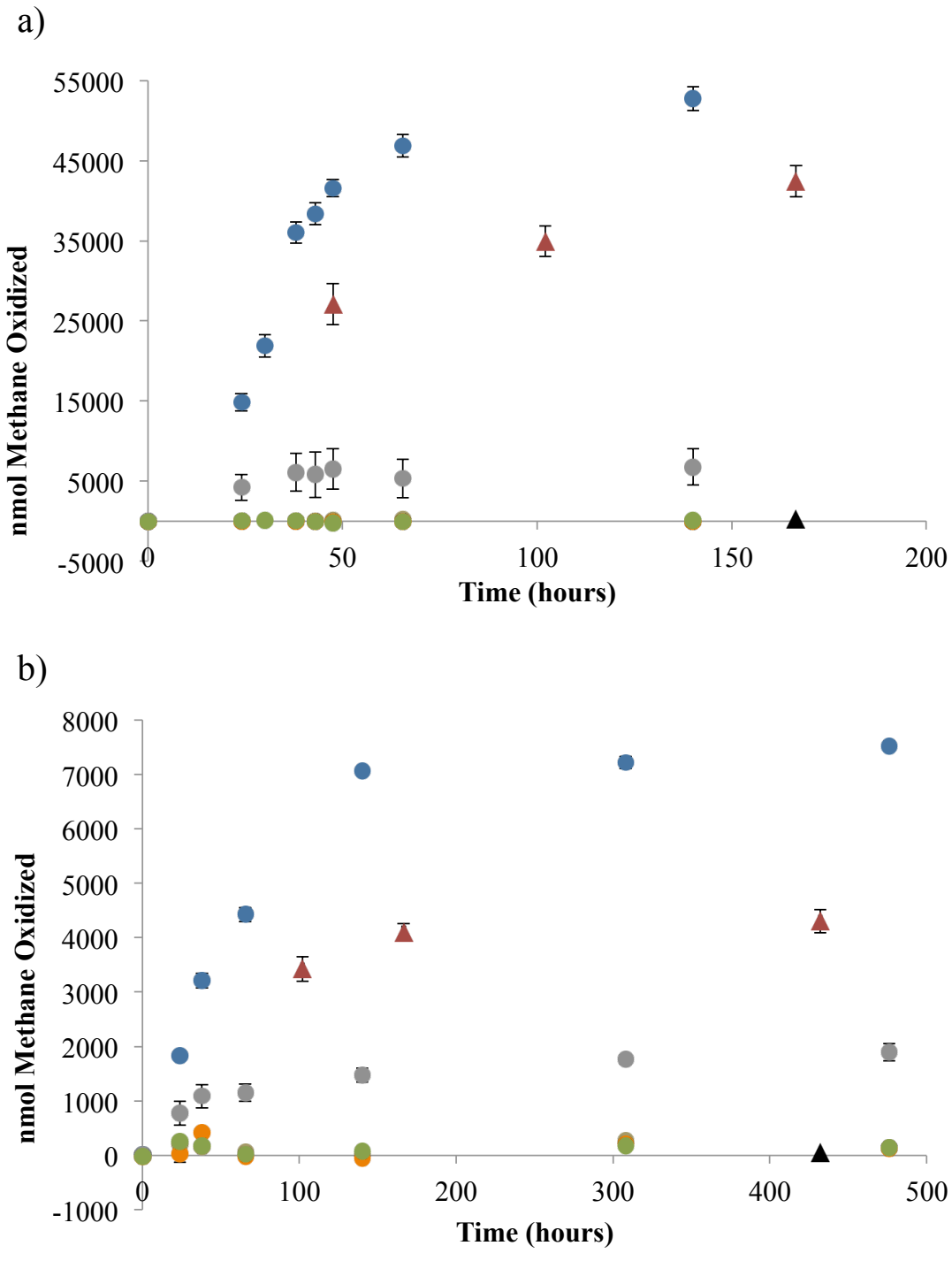

Biogeosciences Discuss., doi:10.5194/bg-2016-202, 2016
Manuscript under review for journal Biogeosciences
Published: 19 May 2016

Figure 2

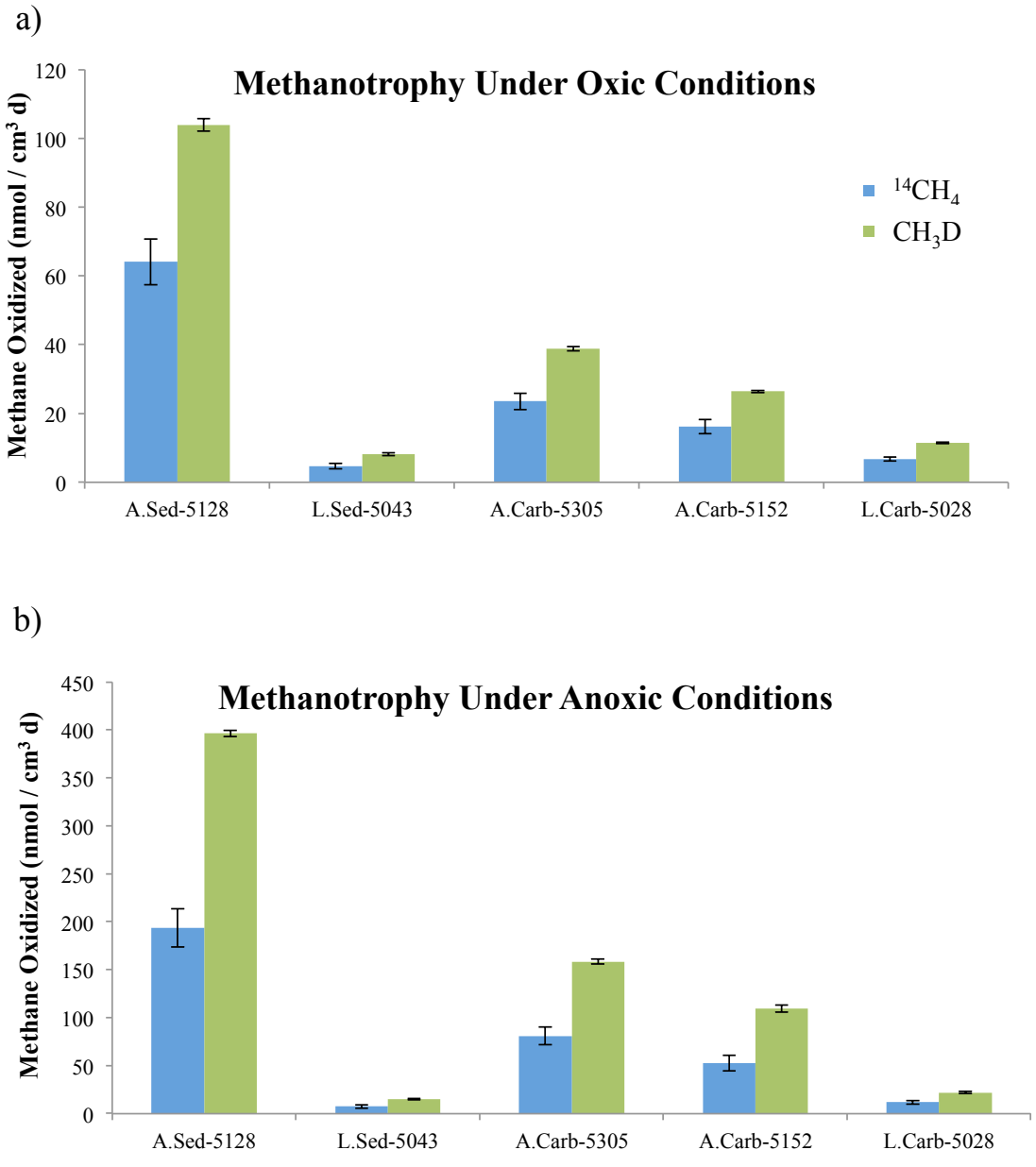

Biogeosciences Discuss., doi:10.5194/bg-2016-202, 2016
Manuscript under review for journal Biogeosciences
Published: 19 May 2016

Figure 3

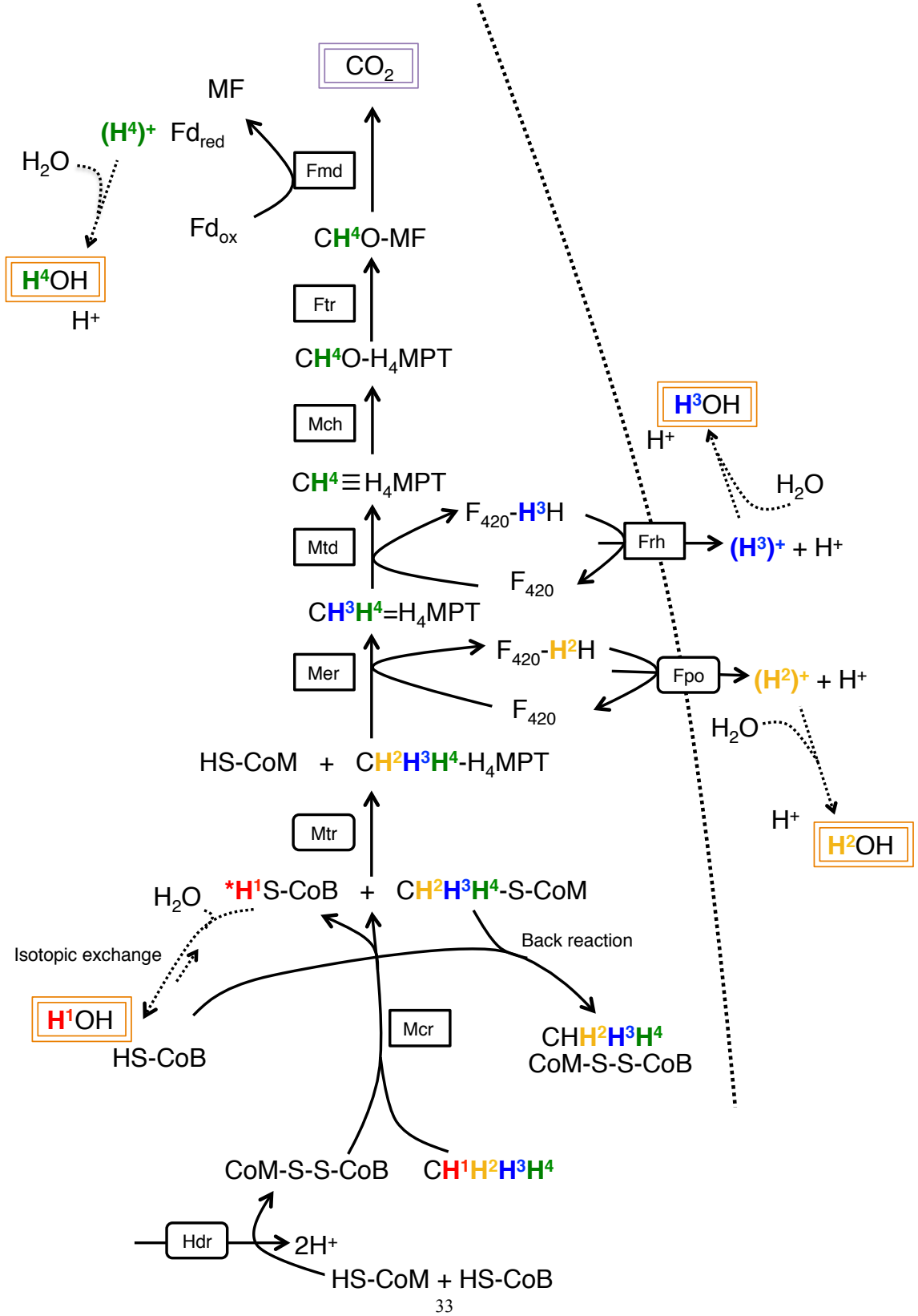

Biogeosciences Discuss., doi:10.5194/bg-2016-202, 2016
Manuscript under review for journal Biogeosciences
Published: 19 May 2016

Figure 4

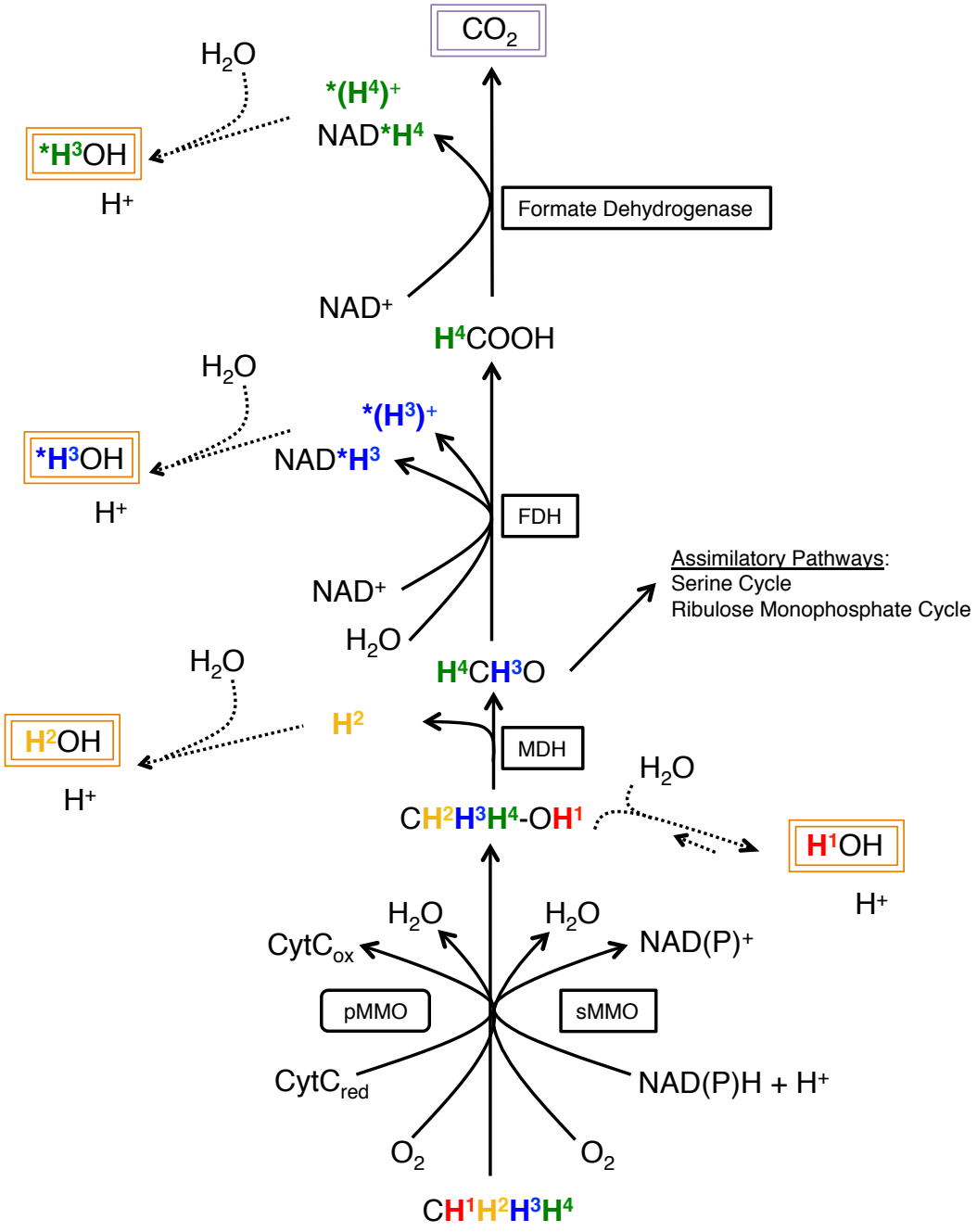

Biogeosciences Discuss., doi:10.5194/bg-2016-202, 2016
Manuscript under review for journal Biogeosciences
Published: 19 May 2016

Figure 5